SnO_2-Nafion® nanocomposite polymer electrolytes for fuel cell applications

S. Brutti*

Dipartimento di Scienze,
Università della Basilicata,
V.le Ateneo Lucano 10, 85100 Potenza, Italy

and

Istituto dei Sistemi Complessi (UOS Sapienza),
Consiglio Nazionale delle Ricerche,
Via dei Taurini, 00185 Roma, Italy
E-mail: sergio.brutti@unibas.it
*Corresponding author

R. Scipioni, M.A. Navarra and S. Panero

Dipartimento di Chimica,
Sapienza Università di Roma,
P.le Aldo Moro 5, 00185 Roma, Italy
E-mail: roscip@dtu.dk
E-mail: mariassunta.navarra@uniroma1.it
E-mail: stefania.panero@uniroma1.it

V. Allodi, M. Giarola and G. Mariotto

Dipartimento di Informatica,
Università di Verona,
strada le Grazie 15, 37134 Verona, Italy
E-mail: valentina.allodi@univr.it
E-mail: marco.giarola@univr.it
E-mail: gino.mariotto@univr.it

Abstract: Fuel cells are capable to exploit the combustion of hydrogen to convert chemical energy into electricity. Polymer electrolyte fuel cells based on Nafion membranes are able to work in a relatively low temperature range (70–90ºC) but require operating relative humidity (RH) close to 100%. To develop proton-exchange membranes with adequate performances at low RH, an attractive strategy consists of the incorporation of inorganic fillers into the host Nafion polymer. Here, we report on the incorporation of SnO_2 nanopowders with high acidic properties as fillers in Nafion-based polymer electrolytes. Nanometre-sized sulphated SnO_2 particles have been synthesised and incorporated in Nafion polymer membranes. Morphological and vibrational properties of the oxides and membranes, as well as their electrochemical behaviour, have been investigated by atomic force microscopy (AFM),

micro-Raman and infra-red (IR) spectroscopies and electrochemical impedance spectroscopy (EIS). The nanocomposite electrolytes have been used to form a membrane-electrodes assembly with commercial Pt-based catalysts and tested in hydrogen fuel cells.

Keywords: SnO_2; surface functionalisation of oxides; Nafion composite membranes; structural, vibrational and morphological characterisation; conductivity and fuel cell tests.

Reference to this paper should be made as follows: Brutti, S., Scipioni, R., Navarra, M.A., Panero, S., Allodi, V., Giarola, M. and Mariotto, G. (2014) 'SnO_2-Nafion® nanocomposite polymer electrolytes for fuel cell applications', *Int. J. Nanotechnol.*, Vol. 11, Nos. 9/10/11, pp.882–896.

Biographical notes: Sergio Brutti obtained his PhD in Chemical Sciences from Sapienza Unviersità di Roma in 2000. His main research interest is on the synthesis and characterisation of advanced nanomaterials for energy conversion and storage.

Roberto Scipioni is a PhD student at Risø Campus, 'DTU Energy Conversion' and his research is focused on the investigation of performance and lifetime-limiting effects in Li-ion batteries.

Maria Assunta Navarra is a Researcher at Sapienza University of Rome. She has her Master's degree in Chemistry and PhD in Material Science. She is focused on the research of functional materials for energy storage and conversion, mainly electrolytes for lithium batteries and fuel cells. She was awarded by the international ENI ITALGAS prize 'Debut in Research' for her studies applied to fuel cell technologies. She is the author of 40 papers and one chapter.

Stefania Panero is an Associate Professor of Physical Chemistry at Sapienza University of Rome, and Director of the Research Centre of Sapienza University of Rome HYDRO-ECO. She has focused her attention on nanotechnology for the development of new types of electrode and electrolyte materials for advanced batteries and fuel cells. Her publications include over 160 papers in international journals, four chapters and six patents.

Valentina Allodi received her Bachelor's degree in Material Science and Master's Degree in Innovative Material Science from the University of Parma in 2008 and in 2010, respectively. She is a second-year PhD student in Nanotechnologies and Nanostructured Materials at the Vibrational Spectroscopy Laboratory of the University of Verona. Her research activity areas are micro-Raman spectroscopy and infrared spectroscopy of solid-state systems, in particular of nanostructured PEM fuel cell components.

Marco Giarola received his Master's degree in Physics from the University of Trento in 2008, and his PhD in Nanotechnology and Nanomaterials from the University of Verona in 2012. He is a Research Associate at the Vibrational Spectroscopy Laboratory of the University of Verona. His main research interests are in micro-Raman spectroscopy and vibrational imaging of solid-state systems (nanostructured semiconductor and composite films). He has co-authored 29 publications in international scientific journals.

Gino Mariotto received his Laurea degree in Physics from the University of Padua in 1974. He became Professor of Experimental Physics at the University of Trento in 2000. Since the end of 2006, he has moved to the University of

Verona, where he developed the local vibrational spectroscopy laboratory. He is the co-author of more than 230 papers in solid-state physics. His research interests include vibrational dynamics of ionic crystals, optical properties of metal transition and rare earth ions in insulators, nanostructured materials (semiconductor and ceramics compounds) and Raman micro-spectroscopy of functional materials (polymers and composites) in form of thick films.

1 Introduction

The pursuit of an eco-compatible and long-term sustainable economic and social development is driving the worldwide R&D efforts in the field of energy storage and conversion. In this view, fuel cells have been at the centre stage in the first decade of the 21st century. These devices are able to exploit the combustion of hydrogen to convert chemical energy directly into electricity with very high efficiencies, much larger compared with internal combustion engines.

Polymer electrolyte fuel cells based on Nafion membranes are capable to work in a relatively low temperature range (70–90ºC) [1,2] but require operating relative humidity (RH) close to 100% to allow effective proton conduction in the polymer electrolyte. For the development of innovative proton-exchange membranes with adequate performances at low relative humidity, an attractive strategy consists of the incorporation of inorganic acidic materials into the host Nafion polymer [3,4]. A promising route is based on the incorporation of nanosized particles of hygroscopic metal oxides, which act as water reservoir in the polymeric matrix. Furthermore, introducing functional groups on the inorganic moieties can be successfully used to enhance the high temperature properties of the resulting composite membrane, including proton conductivity, mechanical stability and resistance to fuel permeability. Sulphated metal oxides and, in particular sulphated zirconium oxide, are actually attracting much interest as fuel cell membrane additives [5–7]. Recently, sulphated tin oxide has been successfully used as an additive in polymer electrolyte membranes for direct methanol fuel cells [8]. In a previous publication [9], we compared the synthesis of SnO_2 nanopowders obtained by different methods and characterised the oxide powders and the corresponding Nafion-composite membranes to highlight the structural, thermal and mechanical alterations owing to the filler incorporation without analysing the resulting performances in real fuel cells.

In this new paper, we report a further detailed characterisation at molecular level of nanosized SnO_2 systems with high acidic properties and their adoption as fillers in Nafion-based polymer electrolytes for fuel cell testing. Nanometre-sized sulphated tin oxide particles have been obtained by a wet chemistry method. Morphological characteristics as well as surface and molecular properties of the obtained compounds have been investigated by several techniques including AFM, Raman and IR spectroscopies. SnO_2 nanomaterials, bare or functionalised with surface sulphate groups, have been incorporated in Nafion polymer membranes through a solvent-casting procedure and the physical–chemical properties of the resulting composite electrolytes have been analysed, to elucidate the effect of the filler in terms of conductivity and molecular features. Wet polymeric membranes have also been characterised by AFM to get insights about the role played by the inorganic fillers in the modification of the

surface nano-morphology. The synthesised innovative nanocomposite electrolytes have been used to form a membrane-electrodes assembly (MEA) with commercial Pt-based catalysts and tested in hydrogen fuel cells at various temperature and RH conditions: the obtained performances exceed in all cases those measured on conventional, recast Nafion-based MEA free from inorganic additives.

2 Experimental details

2.1 Materials synthesis

SnO_2 powders have been obtained in the form of highly hydrated nanosized particles by a wet chemistry synthesis [10]. $SnCl_4$ (Fluka, 99%) has been dissolved in water (2M solution). A measured volume of a concentrated (30% weight) NH_3 water solution (10 ml) has been, therefore, added dropwise to the Sn(IV) solution (20 ml) thus leading to the formation of a white soft $Sn(OH)_4$ colloid. The $Sn(OH)_4$ colloid has been carefully washed with de-ionised water until NH_4^+ and Cl^- residual contaminations were removed. The final white gel has been dried under dynamic vacuum overnight at 110ºC and then hand grinded. The sample has been designated as F110.

The sulphated tin oxide (F110S) has been obtained by chemical treatment of the F110 sample, followed by calcination. The starting oxide has been suspended in de-ionised water and stirred continuously to enhance the water adsorption. After 24 h of vigorous stirring, the water suspension has been treated with H_2SO_4 (final concentration 0.5M) for 30 min under stirring. After decantation, the material has been filtered and then annealed in air for 3 h at 500ºC.

2.2 Preparation of the composite membranes

Both doped- and undoped-Nafion membranes have been prepared following a solution casting procedure. The commercial Nafion solution (5 wt% in water/alcohol, Ion Power Inc. E.W. 1100) has been treated with N,N-dimethylacetamide at 80ºC to replace solvents. When required, inorganic filler powders were added to the Nafion solution and stirred to homogenise the suspension. An optimal additive loading of 5% with respect to the Nafion polymer weight was chosen for our investigations [8]. The mixture has been casted on a Petri dish and dry membranes have been obtained by solvent evaporation at 90ºC. The casted polymer membranes, having a geometrical surface area of ca. 28 cm^2, have been hot-pressed at 175ºC for 15 min at 10 tons to improve robustness and finally activated and purified by subsequent immersions in boiling hydrogen peroxide (3 vol.%), sulphuric acid (0.5M) and water. All the investigated membranes show very similar thicknesses of about 90 μm. Membranes containing the inorganic fillers will be labelled in the text as N-F110 and N-F110S, respectively. Undoped membranes, used as internal benchmark, will be referred to as 'Nafion recast' and labelled as 'N'.

2.3 Experimental methods

The vibrational characterisation of different samples was carried out by means of FT-IR and Raman spectroscopy measurements.

FT-IR spectra were obtained at room temperature in the ATR configuration within the spectral range between 4000 cm^{-1} and 900 cm^{-1} using a JASCO spectrometer (mod. FT/IR-660 plus) equipped with a ceramic source, a KBr beam splitter and a tri-glycine-sulphate (TGS) detector, operated under vacuum conditions. During the measurements, the sample was kept in contact with the flat surface of a Ge crystal by means of a spring to maximise the detectable signal. All the IR spectra were recorded with a resolution of 4 cm^{-1} using a polystyrene film as a reference. The number of scans for each spectrum being automatically chosen and averaged to ensure an optimal signal-to-noise ratio. A proper baseline has been systematically subtracted from all the spectra to make more significant the comparison among them.

Raman spectra were carried out in backscattering geometry at room temperature by means of a micro-sampling set-up (Horiba-Jobin Yvon, model LabRam HR), equipped with a He-Ne laser, as excitation source at 632.8 nm, with a narrow band notch filter, for Rayleigh line cut-off, and with a spectrograph of 80 cm focal length, used to disperse the scattered radiation. The scattered radiation was detected at the spectrograph output by a multichannel detector, a CCD with 1024 × 256 pixels, cooled by liquid nitrogen and the spectral resolution was about 1 cm^{-1}/pixel. The detection limit on the side of low wave-number, due to the notch filter, was about 200 cm^{-1}. The best Raman spectra were obtained by focusing the laser beam onto a spot of about 2 μm in size through the lens of a long-working distance 50X objective, with high numerical aperture (N.A. = 0.50), while the power on the sample surface was kept well below 3 mW. Due to low laser irradiance power and poor Raman cross-section efficiency of the powder sample, long integration time was mandatory to obtain spectra with a reasonable signal-to-noise ratio (S/N). In some cases, cyclic scans were carried out from the same sample micro-region and then averaged to improve the S/N. All the spectra were calibrated in frequency using the emission lines of an Ar spectral lamp. Repeated micro-Raman spectra were carried out under the same experimental conditions from different points of the investigated sample, to verify their reproducibility over its surface. The recorded spectra were processed to remove artefacts due to cosmic rays, while the luminescence background, consisting of a continuous line, having both shape and intensity dependent of the sample region, and underlying the overall Raman spectrum, was subtracted before starting the analysis of the experimental data.

The morphology of membranes has been studied by the Park AFM XE120 instrument in tapping mode (TM). Images have been analysed by the ImageJ software [11,12]. Energy dispersive X-ray spectroscopy analysis has been carried out in a Leo scanning electron microscopy instrument (Oxford Instruments).

Ex situ conductivity measurements were performed by using a screwed porous stainless steel cell where the given membrane sample was sandwiched between two commercial electrodes (BASF, ELAT GDE LT140 EW with a Pt loading of 5 g m^{-2}). This conductivity cell was put in a home-made chamber equipped with a temperature/ relative humidity controller (Vaisala HTM 330 probe). The measurements were carried out at two critical temperatures (i.e., 90ºC and 100ºC) by setting the desired relative humidity level (i.e., RH = 100% and 25%) through the inlet of a saturated hot vapour stream. The conductivity of the given membrane was evaluated from impedance spectra recorded with a Solartron frequency response analyser 1255B by applying a 10 mV signal in the frequency range 100 kHz–1 Hz.

Fuel cell tests were performed by using a compact system (850C, Scribner Associates Inc.) connected to a 5 cm^2 cell fixture. The active surface of the used electrodes (BASF, ELAT GDE LT140 EW with a Pt loading of 5 g m^{-2}) was brushed with a Nafion solution (ca. 0.5 mg dry Nafion cm^{-2}). The membrane-electrode assembly, MEA, was realised by hot pressing the given membrane between two electrodes at 120ºC and 2 atm for 7 min. The cell was fed with H_2 and air at atmospheric pressure according to current-dependent mass flow rates. Accordingly, 1.4 times anode stoichiometric flow and 3.3 times cathode stoichiometric flow were programmed. The humidification of the cell was accomplished by bubbling the fed gases through stainless steel cylinders incorporated in the compact system and containing distilled water. The temperature of the humidifiers, as well as that of the cell, was properly set to achieve the desired relative humidity. The compact fuel cell test system is equipped with an integrated frequency response analyser (880 Impedance Analyser) able to add an AC sine wave to the DC current flowing in the cell, in the frequency range 10 kHz–1 Hz. The amplitude of the sine wave was chosen to be 10% of the DC current flowing at a cell voltage of 0.45 V. In situ impedance spectra were obtained with the integrated frequency response analyser under the same experimental conditions (i.e., cell temperature, relative humidity and reactant gases parameters) used for the polarisation curves.

3 Experimental results

3.1 Inorganic fillers characterisation

A detailed structural analysis of the prepared oxide powders based on X-ray diffraction and scanning electron microscopy investigation is reported in a previous paper by us [9]. Details are here omitted to avoid redundancies. Briefly, almost spherical, hydrated SnO_2 nanoparticles (total H_2O loss at 400ºC between 5 and 15% in weight), having a tetragonal rutile structure and a surface sulphate content of ca. 7% in mass, were obtained. The amount of sulphate groups chemically bonded on the surfaces of the tin oxide particles have also been evaluated by EDX chemical composition analysis. The experimental S/Sn ratio ranges between 0.03 and 0.038 corresponding to an average sulphate group amount of 6.1 ± 1.2% in respect of the total SnO_2 mass.

Turning to the new original vibrational characterisation, the spectral properties of our nanosized powders have been compared with a commercial powder (Sigma-Aldrich, product number 549657) used as benchmark. Figure 1 shows the Raman spectra of samples F110 and F110S, together with that of the commercial SnO_2 powder, nominally in rutile phase. Raman spectrum of crystalline SnO_2 in rutile phase, also named cassiterite, with tetragonal symmetry P42/mnm (space group $D_{14}{}^{4h}$), consists of 4 Raman active modes of $1A_{1g}$, $1B_{1g}$, $1B_{2g}$ and $1E_g$ symmetry, which were observed at B_{1g} (~88 cm^{-1}), E_g (476 cm^{-1}), A_{1g} (638 cm^{-1}) and B_{2g} (782 cm^{-1}), respectively [13,14]. The last three modes are clearly observed in the spectrum of commercial powder (see bottom panel of Figure 1), which also shows a much broader band, with relatively low intensity, peaked at about 566 cm^{-1}, likewise to be ascribed to its amorphous component. In fact, the wavenumber values quoted in this panel perfectly fit the reported ones for nanocrystalline powders SnO_2 characterised by some degree of non-stoichiometry [15].

Figure 1 Unpolarised micro-Raman spectra recorded under excitation at 632.8 nm from the commercial SnO_2 powder (bottom panel), and from the samples F110 (mid panel) and F110S (top panel). Some typical Raman bands of polycrystalline SnO_2 in rutile phase are present in all of the spectra

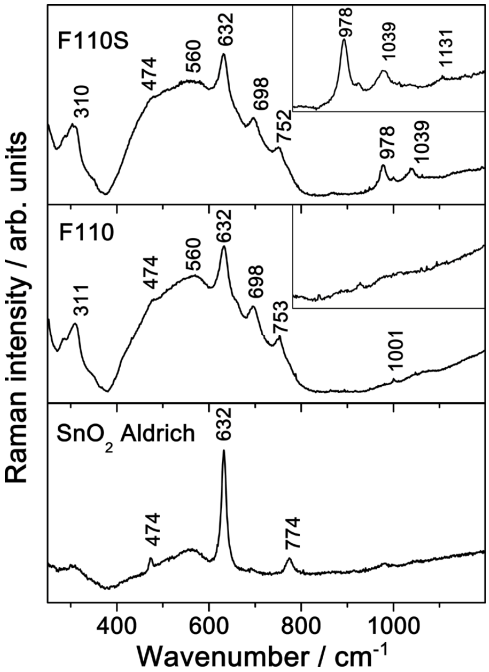

The spectra of the F110 and F110S samples, reported in mid and top panels of Figure 1, display the two characteristic bands of tetragonal rutile SnO_2 at 474 cm^{-1} and 632 cm^{-1}, over-imposed on a much stronger bump centred at about 560 cm^{-1}, which probably hides the missing SnO_2 peak at 774 cm^{-1} and, in the meanwhile, reveals the presence of an important amorphous component in our nanosized powders. In addition, the two spectra show some other common bands, occurring at about 310 cm^{-1}, 698 cm^{-1}, 752 cm^{-1} and 1000 cm^{-1}, of unknown origin, but surely originated by the impurities present in the F110 powder. Finally, the sample F110S also displays three additional peaks at about 978 cm^{-1}, 1039 cm^{-1} and 1131 cm^{-1}, which are characteristic vibrational modes of sulphate (SO_4^{2-}) group [16]. In particular, the peak at 978 cm^{-1} is due to SO_4^{2-} intra-molecular normal mode ν_1, while the two peaks at 1039 cm^{-1} and 1131 cm^{-1} are due to the splitting of the ν_3 mode [16]. The presence of these three peaks in the sulphated sample is confirmed by the FT-IR spectra recorded in ATR configuration on the same sample F110S (see Figure 2, top panel).

In contrast, no evidence of these peaks can be inferred from the corresponding FTIR spectra of commercial powder (Figure 2, bottom panel) or of the sample F110 (Figure 2, mid panel). The splitting of the ν_3 mode in two different components is due to a symmetry lowering of the SO_4^{2-} molecular group suggesting the formation of monodentate sulphate groups coordinated to the tin oxide particles.

Figure 2 ATR spectra recorded in the spectral range between 900 cm^{-1} and 1400 cm^{-1} from the commercial SnO_2 powder (bottom panel) and from the samples F110 (mid panel) and F110S (top panel). The occurrence of three distinct peaks in the spectrum of sample F110S suggests the formation of monodentate sulfate groups

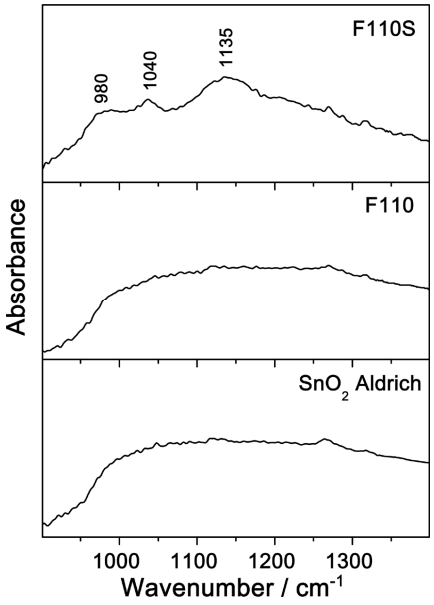

3.2 Membranes characterisation

The morphology of the Nafion-recast and the composite membranes has been investigated by AFM in tapping mode recording topographies and phase images. Membranes have been studied in air at room temperature at 100% relative humidity, after a 12 h swelling in deionised water. The topographies and the corresponding 3D reconstructions are shown in Figure 3.

The morphology of the surfaces of all the three membranes is homogeneous and shows the expected regular undulations over the *z*-axis due to the alternation of hydrophilic and hydrophobic domains. The two composite membranes show both smoother surfaces compared with the Nafion recast. Furthermore, the apparent *x*-*y* linear periodicity of the *z*-axis surface undulations decreases passing from the Nafion recast (9.4 ± 0.4 nm) to the N-F110 (8.8 ± 0.2 nm) and the N-F110S (8.1 ± 0.3 nm) membranes. Such trend suggests the contraction of the size of the hydrophilic domains in the composite membranes compared with the simple Nafion recast. These evidences are possible clues of an alteration of the ability of the composite membranes to bond physisorbed water within the hydrophilic domains close to the surface. One may suggest that the incorporation of the inorganic fillers leads, during the recast procedure, to the formation of smaller ionic domains in proximity of the surface thus improving the homogeneity of the surface hydration.

Turning to the role played by the inorganic filler, it is interesting to observe that the AFM tapping mode phase images of the surface of the composite membranes show a good dispersion of the SnO_2 particles on the surface. As an example, the phase image of the surface of the N-F110 membrane is shown in Figure 4.

Figure 3 AFM topographies and 3D reconstructions of the three studied membranes recorded in air at room temperature with RH = 100%

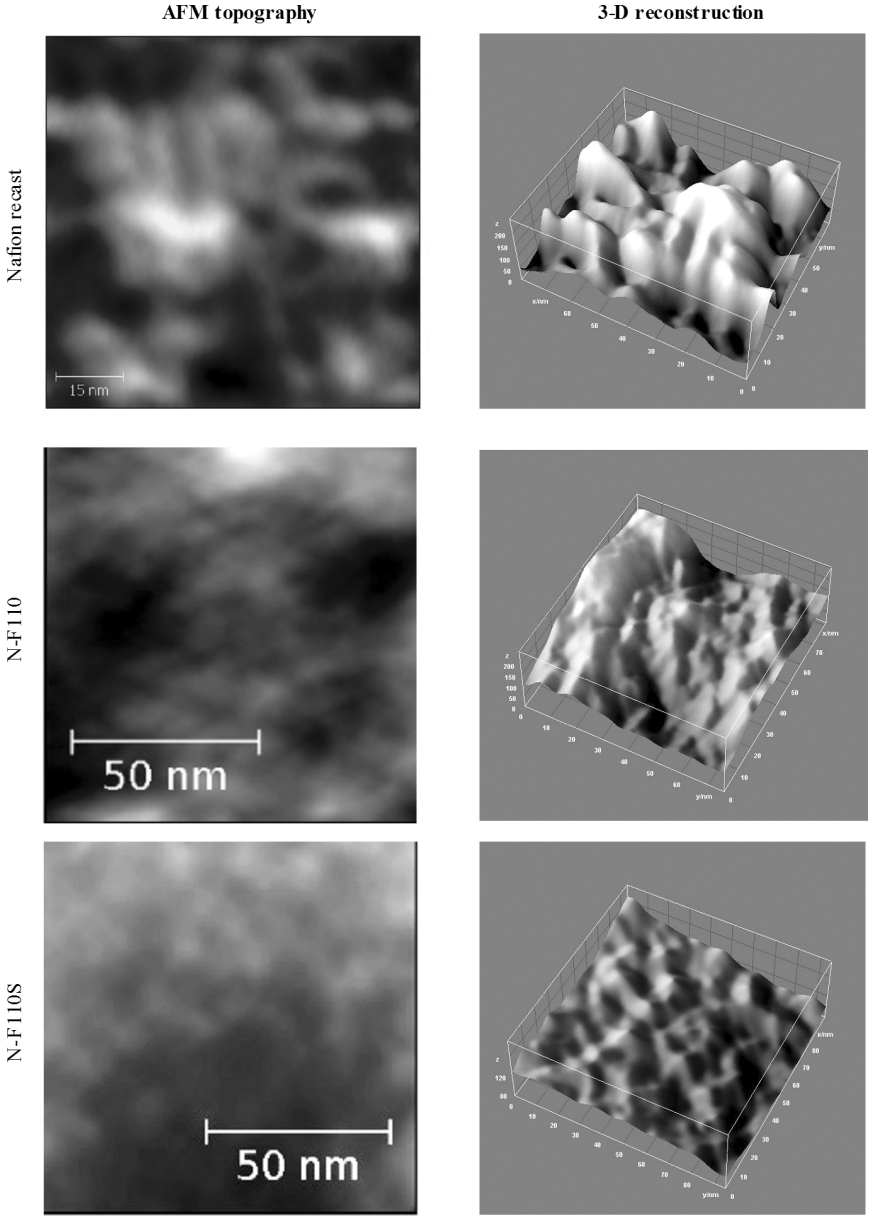

The phase signal is sensitive to many different factors and in particular in the case of composite materials to surface variations in composition due to abrupt chance of the elastic properties. The overall phase response of the surface of the N-F110 membrane shows moderate contrast undulations (light areas) easily related to the alternation of the hydrophilic–hydrophobic domains. The few isolated dark spots that can be observed in Figure 4 are likely due to the inorganic filler nanoparticles. These dark round-shaped

particles show a mean linear size of approximately 17.0 ± 1.4 nm thus suggesting the limited agglomeration of few SnO_2 nanoparticles within the membranes.

The vibrational characterisation of the Nafion membranes, both without and with the inorganic filler, has been carried out either by Raman spectroscopy or by IR measurements.

Typical micro-Raman spectra of composite membranes (N-F110 and N-F110S) are reported in Figure 5, together with the spectrum of Nafion recast, used as reference.

Figure 4 AFM phase image of the N-F110 membrane recorded in air at room temperature with RH = 100%

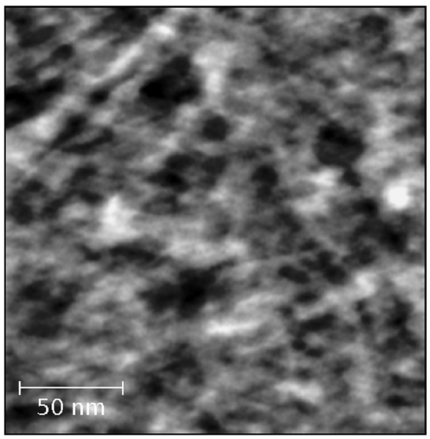

Figure 5 Unpolarised micro-Raman spectra recorded under excitation at 632.8 nm from the pure Nafion membrane (bottom panel), and from the membranes N-F110 (mid panel) and N-F110S (top panel)

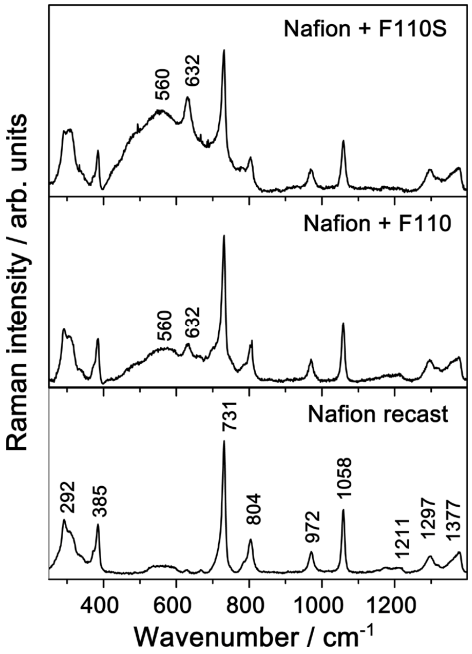

On pure Nafion membrane (Nafion recast), several characteristic bands of the Nafion are observed at about 300 cm^{-1} [$t(CF_2)$], 385 cm^{-1} [$\delta(CF_2)$], 570 cm^{-1} [$\delta(CF_2)$], 730 cm^{-1} [$v_s(CF_2)$], 805 cm^{-1} [v(C–S)], 970 cm^{-1} [v_s(C–S)], 1058 cm^{-1} [$v_s(SO_3^-)$], 1210 cm^{-1} [$v_{as}(CF_2)$], 1297 cm^{-1} [v(C–C)] and 1380 cm^{-1} [v_s(C–C)]. These peaks correlate quite well with results obtained by Gruger et al. [17] on Nafion membranes by means of a joint IR and Raman study. Both samples N-F110 and N-F110S show a more complex spectrum resulting from the superposition of the Nafion membrane spectrum with that of the nanosized SnO_2 powder, with no clear evidence of spectral features related to sulphate group.

The presence of tetragonal rutile SnO_2, both in crystalline and in amorphous phases, in the two composite samples, is revealed by the two peaks at 632 cm^{-1} and 474 cm^{-1} (this last hardly observable) overlapping the broad band at about 560 cm^{-1}, while no apparent new Raman mode is observed, which could suggest an interaction between the filler and the host matrix. This finding, therefore, confirms the composite nature of our N-F110 and N-F110S samples, and the apparent absence of an evident chemical affinity between these two components.

This picture is confirmed by a comparative FT-IR analysis of the three different samples. In fact, their ATR spectra observed in the spectral range between 900 cm^{-1} and 1400 cm^{-1}, shown in Figure 6, do not evidence any appreciable modification due to the incorporation of the nanosized powder in the Nafion membrane, apart may be a hardly observable broadening of the vibrational stretching mode $v_s(SO_3^-)$ at about 1060 cm^{-1}.

Figure 6 ATR spectra recorded in the spectral range between 900 cm^{-1} and 1400 cm^{-1} from the pure Nafion membrane (bottom panel), and from the membranes N-F110 (mid panel) and N-F110S (top panel)

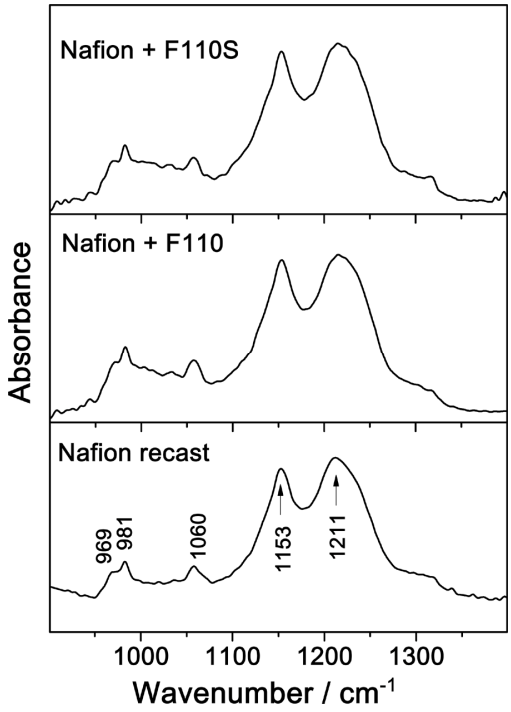

Proton conductivity of both plain and doped membranes has been evaluated under critical temperature values (i.e., 90ºC and 100ºC) by moving from ideal, fully hydrated conditions (i.e., RH = 100%) to very low, severe humidity levels (i.e., RH = 25%). The results of this measurement are reported in Figure 7.

Figure 7 Conductivity of the three investigated membranes

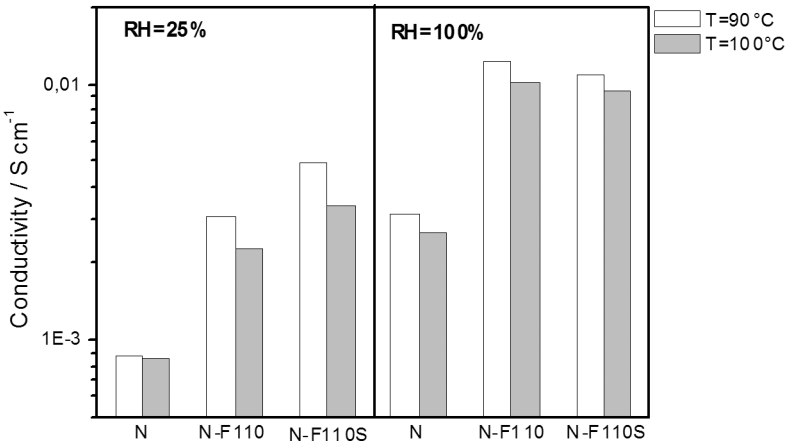

All the investigated membranes experience a decay of conductivity, even if very small in some cases, with temperature. This result can be related to a structural change occurring in the Nafion polymer matrix around 90ºC [18,19] and reveals that the selected inorganic fillers do not play any significant role in affecting such polymer transition. The two composite membranes show much higher conductivity with respect to undoped Nafion and a strong reduction of proton conductivity is observed for all the samples when the humidity content is decreased down to RH = 25%. Under this strict condition, the N-F110S sample displays the best behaviour and its conducting ability is still acceptable. This evidence can be ascribed to an improved water affinity/retention of the quoted membrane despite the low, external humidity level, this positively affecting proton transport throughout the hydrophilic ionic cluster of the polymer and the oxide surface.

N-F110S membrane was selected to drive fuel cell tests aimed at elucidating the applicability of the proposed electrolyte under critical operating conditions. Relative high cell temperature (i.e., 90ºC) was considered, being the set value the limit where undoped, conventional Nafion membranes normally fail. Polarisation and power density curves are reported in Figure 8.

Even if current and power delivered were not of high practical interest, being this partly related to a non-optimised experimental set-up, the functionality of the membrane was proved and fuel cell tests under very ‘dangerous’ parameters (i.e., 90ºC and 25% RH) were possible. In-situ impedance measurements, recorded at 0.45 V and displayed in Figure 9 in the form of Nyquist plots, account for the various resistive phenomena occurring within the MEA. It is reasonable to assume that the high-frequency intercept on the real axis (left end-point of the spectrum) is equal to the total, non-electrode ohmic resistance of the cell, while that at the low frequency (right end-point of the spectrum) is representative of the charge transfer resistance. It is clear that under low relative humidity a deep modification of the spectrum occurs, corresponding to a more complex charge

transference process having a higher associated resistance; as expected, the ohmic resistance is also increased when moving from 100% to 25% RH. The increased amplitude of the semi-circle and its modified shape at low humidification levels can be related to a deterioration of the membrane-electrode interface contact due to the ionomer shrinkage [4,20]. If compared with previous impedance results obtained under comparable testing conditions for cells adopting other hybrid Nafion-based membranes [21], the overall spectrum recorded at 100% RH is slightly worse than expected, mainly in terms of total charge transference resistance, this probably accounting for the quite low, absolute performance shown in Figure 8.

Figure 8 Polarisation and power density curves recorded under fuel cell operation at 90ºC when using the N-F110S membrane as electrolyte

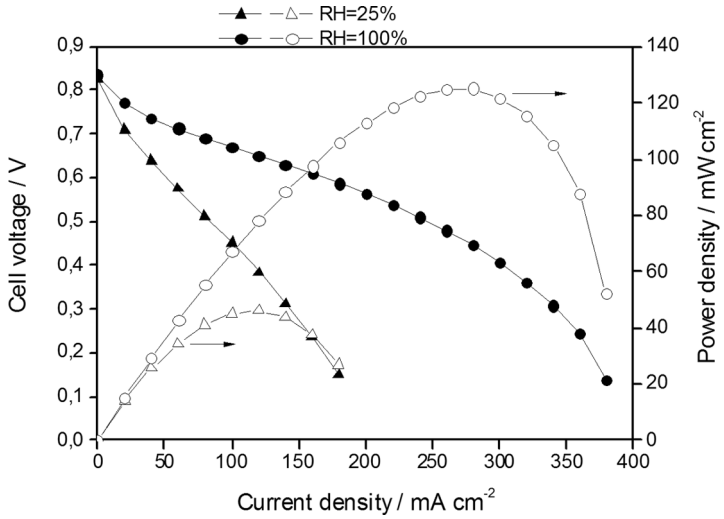

Figure 9 In-situ impedance spectra recorded at 90ºC under fuel cell operation at a voltage of 0.45 V when using the N-F110S membrane as electrolyte

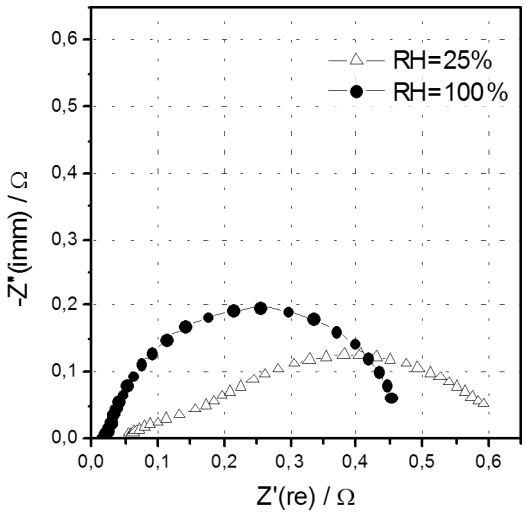

4 Conclusions

Nanocomposite Nafion-based membranes have been synthesised by incorporating nanometric SnO_2 powders without and with surface functionalisation with sulphate groups. Morphological and spectroscopic characterisation of these membranes has been carried out by comparing their properties with a benchmark Nafion recast membrane. No direct evidence of a direct chemical interaction between the filler and the host polymeric network was obtained at molecular level by vibrational spectroscopy. Despite this, a clear alteration at the nanoscale of the membrane morphology was observed by atomic force microscopy. It is likely that these modifications are driven by an improved ability of the composite membranes to bond physisorbed water within the hydrophilic domains. Apparently, the incorporation of the inorganic fillers during the recast procedure induces the formation of smaller and more interconnected ionic domains in proximity of the surface thus improving the homogeneity of the surface hydration. The alteration of the surface morphology and the improved hydration reflects on the ability of these composite membranes to conduct protons and to operate in fuel cells under very critical conditions (i.e., 90ºC and 25% RH) where conventional, recast Nafion normally fails.

Acknowledgement

This work has been performed in the framework of the NAMED-PEM Project "Advanced nanocomposite membranes and innovative electrocatalysts for durable polymer electrolyte membrane fuel cells" (PRIN 2010-2011, prot. 2010CYTWAW_001), funded by the Italian Ministry of University and Research.

References

1 Savadogo, O. (1998) 'Emerging membranes for electrochemical systems: (I) solid polymer electrolyte membranes for fuel cell systems', *J. New Mater. Electrochem. Syst.*, Vol. 1, p.47.

2 Wilkinson, D.P., Zhang, J., Hui, R., Fergus, J. and Li, X. (2010) *Proton Exchange Membrane Fuel Cells: Materials Properties and Performance*, CRC Press Inc., Boca Raton, FL.

3 Ramani, V., Kunz, H.R. and Fenton, J.M. (2005) 'Stabilized heteropolyacid/nafion composite membranes for elevated temperature/low relative humidity PEFC operation', *Electrochim. Acta*, Vol. 50, pp.1181–1187.

4 Thampan, T.M., Jalani, N.H., Choi, P. and Datta, R. (2005) 'Systematic approach to design higher temperature composite PEMs', *J. Electrochem. Soc.*, Vol. 152, pp.A316–A325.

5 D'Epifanio, A., Navarra, M.A., Christoph Weise, F., Mecheri, B., Farrington, J., Licoccia, S. and Greenbaum, S. (2010) 'Composite nafion/sulfated zirconia membranes: effect of the filler surface properties on proton transport characteristics', *Chem. Mater.*, Vol. 22, pp.813–821.

6 Navarra, M.A., Abbati, C. and Scrosati, B. (2008) 'Properties and fuel cell performance of a nafion-based, sulfated zirconia-added, composite membrane', *J. Power Sources*, Vol. 183, pp.109–113.

7 Navarra, M.A., Croce, F. and Scrosati, B. (2007) 'New, high temperature superacid zirconia-doped Nafion™ composite membranes', *J. Mater. Chem.*, Vol. 17, pp.3210–3215.

8 Chen, F., Mecheri, B., D'Epifanio, A., Traversa, E. and Licoccia, S. (2010) 'Development of nafion/tin oxide composite MEA for DMFC applications', *Fuel Cells*, Vol. 10, pp.790–797.

9 Scipioni, R., Gazzoli, D., Teocoli, F., Palumbo, O., Paolone, A., Ibris, N., Brutti, S. and Navarra, M.A. (2014) 'Preparation and characterization of nanocomposite polymer membranes containing functionalized SnO_2 additives', *Membranes*, Vol. 4, pp.123–142.

10 Giesekke, W., Gutowsky, H.S., Kirkov, P. and Laitinen, H.A. (1967) 'A proton magnetic resonance and electron diffraction study of the thermal decomposition of tin(IV) hydroxides', *Inorg. Chem.*, Vol. 6, pp.1294–1297.

11 Abramoff, M.D., Magalhães, P.J. and Ram, S.J. (2004) 'Image processing with image', *Biophotonics International*, Vol. 11, pp.36–42.

12 Rasband, W.S. (1997) *ImageJ*, U.S. National Institutes of Health, Bethesda, Maryland, USA, http://imagej.nih.gov/ij/, 1997–2011.

13 Scott, J. (1970) 'Raman spectrum of SnO_2', *J. Chem. Phys.*, Vol. 53, pp.852–853.

14 Peercy, P.S. and Morosin, B. (1973) 'Pressure and temperature dependences of the Raman-active phonons in SnO_2', *Phys. Rev. B*, Vol. 7, pp.2779–2786.

15 Yu, K.N., Xiong, Y., Liu, Y. and Xiong, C. (1997) 'Microstructural change of nano-SnO_2 grain assemblages with the annealing temperature', *Phys. Rev. B*, Vol. 55, pp.2666–2671.

16 Nakamoto, K. (1986) *Infrared and Raman Spectra of Inorganic and Coordination Compounds*, Wiley and Sons, New York.

17 Gruger, A., Régis, A., Schmatko, T. and Colomban, Ph. (2001) 'Nanostructure of Nafion® membranes at different states of hydration: an IR and Raman study', *Vib. Spectrosc.*, Vol. 26, pp.215–225.

18 Teocoli, F., Paolone, A., Palumbo, O., Navarra, M.A., Casciola, M. and Donnadio, A. (2012) 'Effects of water freezing on the mechanical properties of nafion membranes', *J. Polym. Sci., Part B: Polym. Phys.*, Vol. 50, pp.1421–1425.

19 Giffin, G.A., Piga, M., Lavina, S., Navarra, M.A., D'Epifanio, A., Scrosati, B. and Noto, V.D. (2012) 'Characterization of sulfated-zirconia/Nafion® composite membranes for proton exchange membrane fuel cells', *J. Power Sources*, Vol. 198, pp.66–75.

20 Kanamura, K., Morikawa, H. and Umegaki, T. (2003) 'Observation of interface between Pt electrode and nafion membrane', *J. Electrochem. Soc.*, Vol. 150, pp.A193–A198.

21 Navarra, M.A., Abbati, C., Croce, F. and Scrosati, B. (2009) 'Temperature-dependent performances of a fuel cell using a superacid zirconiadoped nafion polymer electrolyte', *Fuel Cells*, Vol. 3, pp.222–225.